Mon. Not. R. Astron. Soc. **391,** 1350–1358 (2008) doi:10.1111/j.1365-2966.2008.13975.x

The structure of the inner Oort cloud from the simulation of its formation for 2 Gyr

G. Leto,[1⋆] M. Jakubík,[2⋆] T. Paulech,[3] L. Neslušan[2⋆] and P. A. Dybczyński[4⋆]

[1]*Catania Astrophysical Observatory, Via Santa Sofia 78, I-95123 Catania, Italy*
[2]*Astronomical Institute of the Slovak Academy of Sciences, 05960 Tatranská Lomnica, Slovakia*
[3]*Astronomical Institute of the Slovak Academy of Sciences, Dúbravská cesta 9, 84504 Bratislava, Slovakia*
[4]*Astronomical Observatory of the A. Mickiewicz University, Słoneczna 36, 60-286 Poznań, Poland*

Accepted 2008 September 16. Received 2008 September 3; in original form 2008 July 25

ABSTRACT

Considering the model of the initial disc of planetesimals consisting of 10 038 test particles, we simulated the formation of the distant comet reservoirs up to 2 Gyr. The result concerning the outer part of the Oort cloud (OC) was described in our previous paper. Here, we deal with the evolution of the population and structure at 2 Gyr of the complementary inner part of the OC. The dynamical evolution of the massless test particles was followed via the numerical integration of their orbits. We considered the perturbations produced by four giant planets assuming they have their current orbits and masses, as well as the perturbations caused by the Galactic tide and passing stars. The efficiency of the formation of inner OC is found to be very low: only about 1.1 per cent of all considered particles ended in this part of the comet cloud. In particular, the particles originated from Uranus (35.5 per cent), Neptune (35.4 per cent) and Edgeworth–Kuiper belt (18.4 per cent) regions of the initial protoplanetary disc. At 2 Gyr, the dynamics of the inner cloud is mainly governed by the dominant z-term of the Galactic tide. The number density of the bodies is proportional to the heliocentric distance, r, as $\propto r^{-3.53}$. The directional distribution of orbits is still strongly inhomogeneous. There are, for example, large empty regions in the space angles around the Galactic Equator points with the galactic longitude 90° and 270° (non-rotating frame), or there are only few bodies having the ecliptical latitude higher than +60° or lower than −60°. A strong concentration of objects at the ecliptic is apparent up to ≈1000 au (with a possible, but not exactly proved extension to ≈1500 au). Beyond $r \approx 6000$ au, the bodies directly above and below the Sun, with respect to the ecliptic, are absent.

Key words: comets: general – Oort cloud – Solar system: formation.

1 INTRODUCTION

Dynamically, *new* comets are those observed in the zone of visibility, which were not significantly perturbed by the planets during their former revolution around the Sun. They come from the outer part of the comet Oort cloud (OC), which is thus observationally detectable. The researchers noted that the original (before entering the planetary region) semimajor axes of new comets were not shorter than a typical lower limit a_c. Hills (1981) suggested that this inner limit was due to an observational constraint. In the real Solar system, the comet cloud does not have such discontinuity and, most likely, it continually extends inward. This hypothetical part of the comet cloud, which cannot be detected by the direct observation of incoming comets, is referred to as *inner OC*, at present.

⋆E-mail: gle@astrct.oact.inaf.it (GL); mjakubik@ta3.sk (MJ); astrotom@savba.sk (TP); ne@ta3.sk (LN); dybol@amu.edu.pl (PAD)

In our previous work (Dybczyński et al. 2008, hereafter Paper I), we performed a simulation of the OC formation considering massless test particles (TPs). The approximation of real planetesimals or cometary nuclei with massless particles allows us to use the GRID computing technique, with a number of mutually independent CPUs that are more easily accessible than a supercomputer. In our Paper I simulation, we considered the model of the initial disc of planetesimals consisting of 10 038 TPs and studied their dynamics during 1 Gyr, under the influence of the perturbations caused by the four giant planets (on their current orbits and with their current masses), Galactic tide and nearby passing stars. A more detailed description of the initial conditions and computational procedure used can be found in Paper I, where we described the formation and some structural characteristics of the outer part of the OC.

In this work, we extend the simulation time to 2 Gyr and describe the formation process, further dynamical evolution and some features of the structure of the up-to-date hypothetical inner part of the

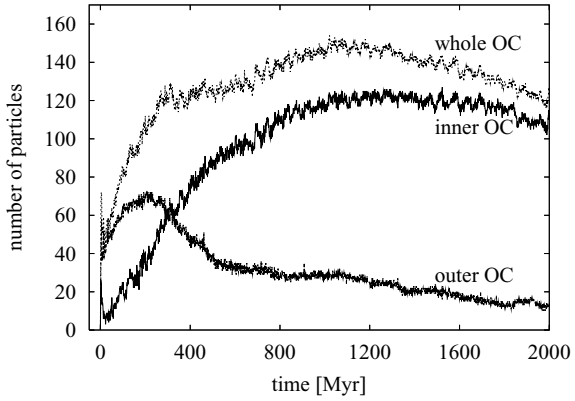

Figure 1. The evolution of the population of the OC during the first 2 Gyr. The evolution of inner OC, outer OC, as well as whole OC populations is demonstrated.

Table 1. The end states, at 2 Gyr, of the TPs, which resided in various regions (the first column) of the PPD at the beginning of the performed simulation. In the beginning, we consider the PPD consisting of 10 038 TPs. In the end of the simulation, some of the TPs, from the given part of planetary region, still have their perihelion, q, in this region, i.e. $q < 50$ au, or they are moved into the inner OC (IOC) or outer OC (OOC), *ejected* into the interstellar space, or are destroyed during a *collision* with one of the considered massive bodies, mostly with the Sun. An asterisk indicates the average values in the period 1991–2000 Myr, since the numbers still vary, in these cases.

Region	$q < 50$	In IOC*	In OOC*	Ejected	Collided
Jupiter	50	4.9	2.0	1389	187
Saturn	13	6.9	1.0	1802	260
Uranus	62	39.0	3.3	1596	367
Neptune	173	38.9	3.0	1443	390
EKB	1734	20.2	3.3	439	122

OC, which, in our research, appeared to form much slower than the outer one (see Fig. 1).

2 THE INNER OORT CLOUD DESCRIPTION AS OBTAINED BY OUR SIMULATION

2.1 Introduction remarks

We classify a given TP as a member of the inner OC, if its perihelion distance is $q \geq 50$ au and its semimajor axis is $2000 < a \leq a_c$, where we adopt $a_c = 25\,000$ au.

It is worth noting that the critical semimajor axis a_c, representing the border between the inner and outer OC, is difficult to be determined by both observations and theory. It should be large enough so that the outer perturbers of the OC, especially the dominant and permanently acting Galactic tide, are sufficient to reduce the comet perihelia from the region beyond the relatively strong Jupiter and Saturn perturbations to the zone of visibility within a single orbit. Hills (1981) suggested $a_c = 20\,000$ au. Here, we must note that at that time astronomers used to consider the value $\rho_{GM} = 0.185\,M_\odot\,pc^{-3}$ (Bahcall 1984) of the Galactic matter density. Recently, a more reliable value $\rho_{GM} \approx 0.1\,M_\odot\,pc^{-3}$ (Pham 1997; Crézé et al. 1998; Holmberg & Flynn 2000) was determined on the basis of the *Hipparcos* observations. It is well known that a lower ρ_{GM} implies a larger value a_c.

During several decades in the past, all comets having the original reciprocal semimajor axis lower than $1 \times 10^{-4}\,au^{-1}$ were regarded as new and, therefore, coming from the outer OC. This criterion was invalidated by Dybczyński (2001) who demonstrated that 41 of 85 comets, classified as new by the above criterion, were significantly perturbed by the planets at their previous perihelion passage. Consequently, if we want to find a characteristic border between the inner and outer OC in terms of semimajor axis, which is naturally implied by a disappearance of truly new comets in observational data, we should take these facts into account and shift a_c to a larger value than that corresponding to $1/a_c = 10^{-4}\,au^{-1}$ or even larger than 20 000 au corresponding to $\rho_{GM} = 0.185\,M_\odot\,pc^{-3}$. In this work, we accept the result published in the recent study by Dybczyński (2006) who demonstrated that observed dynamically new comets have semimajor axes that are greater than 25 000 au if the $\rho_{GM} = 0.1\,M_\odot\,pc^{-3}$ value of the local Galactic matter density is used.

A study of the dynamics of inner-OC bodies can be complicated by the requirement of a very long period of numerical integration of their orbits. It is well known that the dominant outer perturbation due to the z-term of the Galactic tide causes the periodic variations of the orbital elements. The period of these variations is proportional to the semimajor axis as $\propto a^{-3/2}$ (Heisler & Tremaine 1986). The orbital elements of the inner-OC comets can vary with a period much exceeding the age of the Solar system. (In the outer OC, on the contrary, periods can be as short as 1 Gyr.) Due to this circumstance, we do not attempt to extrapolate our results for the period of the first 2 Gyr up to the current inner OC. Nevertheless, the found results can still be interesting, because this first period was important for the occurrence of all characteristic evolutionary features.[1]

2.2 Formation of the inner Oort cloud

The evolution of the inner-OC population is shown in Fig. 1. The maximum population occurs at about 1250 Myr. At the end of our simulation, corresponding to the time of 2 Gyr, this population is represented by 110 TPs that imply 1.1 per cent efficiency of the inner-OC formation. At this time, the population of the outer OC is represented only by about 13 TPs (0.13 per cent formation efficiency). One can calculate that only 10 per cent of the TPs in the OC reside in its outer part at 2 Gyr. These figures are different from the corresponding values obtained in analogous simulations by Duncan, Quinn & Tremaine (1987) or Dones et al. (private communication; Dones et al. 2004). Duncan et al. obtained the efficiency of ≈20 per cent and Dones et al. (private communication) obtained the value of 2.7 per cent in their *cold* and 3.5 per cent in their *hot run* for the inner OC. However, several parameters in our models of the initial protoplanetary disc (PPD) and stellar perturbations as well as our definitions and covered time interval are different, therefore the direct comparison is impossible.

All end states at 2 Gyr are summarized in Table 1 by the region of the initial PPD, in which the TPs originated. (The specific regions

[1] The electronic form of output data from the numerical integration of TP orbits, recorded every mega-year of the dynamical evolution, is available at: http://www.ta3.sk/~mjakubik/AstroDyn/INNER_OC_FORMATION/anims.php for the period from 1 to 2 Gyr. The animations of the evolution of distributions plotted in Figs 3 to 11, for the entire period from 0 to 2 Gyr, are also available on this web site. The output data for the period from 0 to 1 Gyr are available on the web page http://www.ta3.sk/~ne/OUTER_OC_FORMATION/anims.php linked to Paper I.

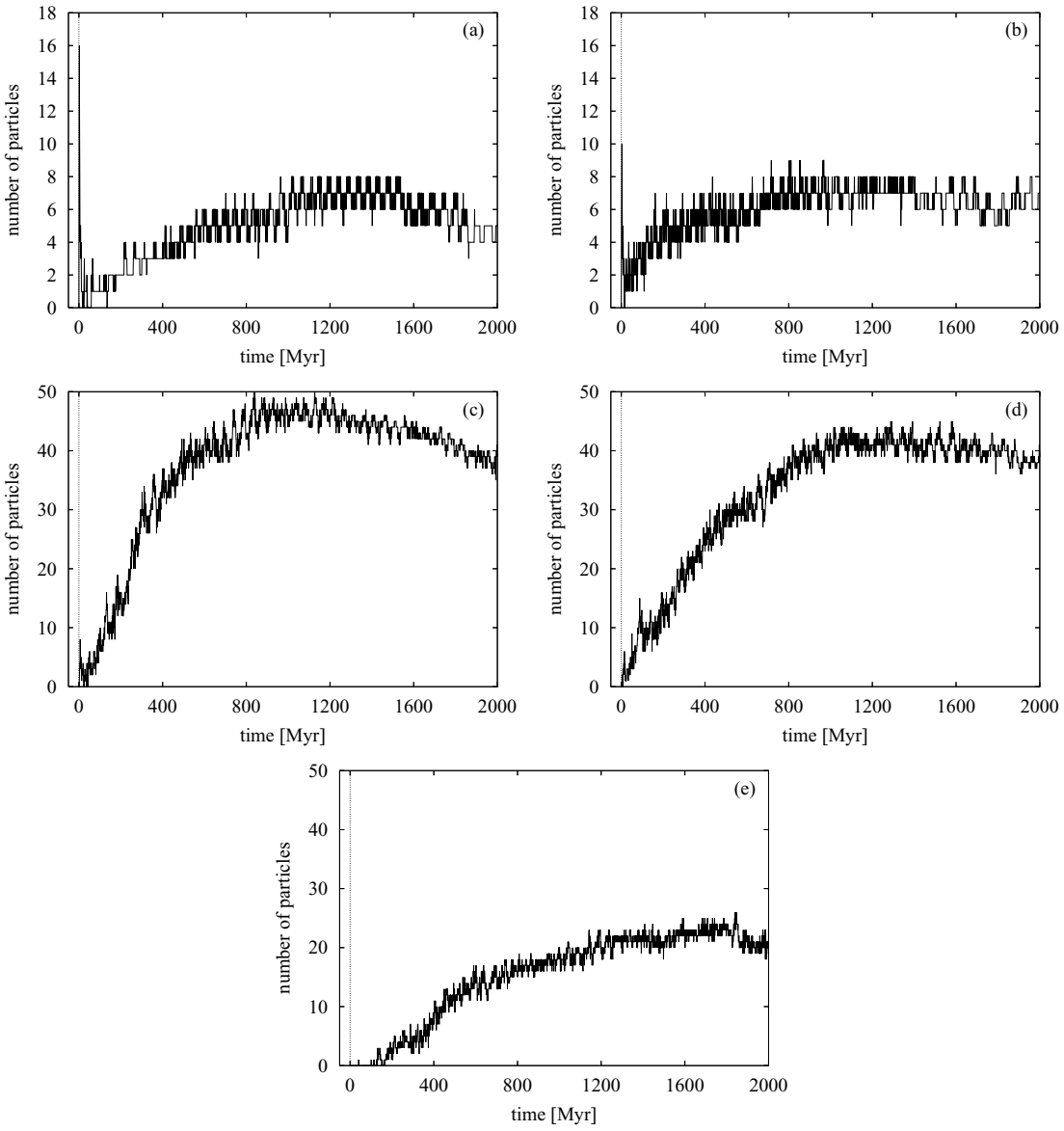

Figure 2. The evolution of the delivery of comets to the inner OC, which initially originated in the Jupiter (plot a), Saturn (plot b), Uranus (plot c), Neptune (plot d) and EKB (plot e) regions. Note the different vertical scale.

of the initial PPD were exactly defined in Paper I, Section 2.1.) The contributions to the inner OC from the individual regions are 4.5, 6.3, 35.5, 35.4 and 18.4 per cent from the Jupiter, Saturn, Uranus, Neptune and Edgeworth–Kuiper belt (EKB) regions, respectively. The evolution of these contributions is also illustrated in Fig. 2. The listed amounts are similar to those of the outer OC (Paper I), besides the expected lower amount of the TPs from Jupiter–Saturn region in comparison with the Uranus–Neptune region. The distribution of the TPs situated in the inner OC at 2 Gyr by the region of their origin is also shown in Fig. 3 (full bars). In contrast to the formation of the outer OC, a lot of TPs reached the inner OC coming from the initial heliocentric distance of 35–37 au. This location corresponds to the 4:3 mean-motion resonance with Neptune. The transiting population of bodies, which have occurred sometime during the 2 Gyr evolution in the inner OC, is illustrated with the empty bars in Fig. 3.

2.3 The radial structure of the inner OC

The radial distribution, its differential and cumulative versions, of the TPs at several selected evolution moments is illustrated in Figs 4 and 5, respectively. To see these inner-OC distributions in a wider context, we plot the radial distribution in Fig. 4 for the entire studied region from 0 to 100 000 au and the cumulative distribution function in Fig. 5 for the 100–100 000 au interval. The behaviour of the radial distribution of the TPs in the inner cloud is rather chaotic during the early stage of its formation (Fig. 4a–d). Only when the inner-OC population approaches its maximum, at ≈1250 Myr, and after the maximum, the inner cloud becomes more and more centrally concentrated. The number density of the TPs residing in the OC in the interval $5000 < r < 100\,000$ au at 2 Gyr can be fitted by the power law with the index of slope $s = -3.529^{+0.031}_{-0.024}$. (The corresponding behaviour of the heliocentric-distance distribution is illustrated with

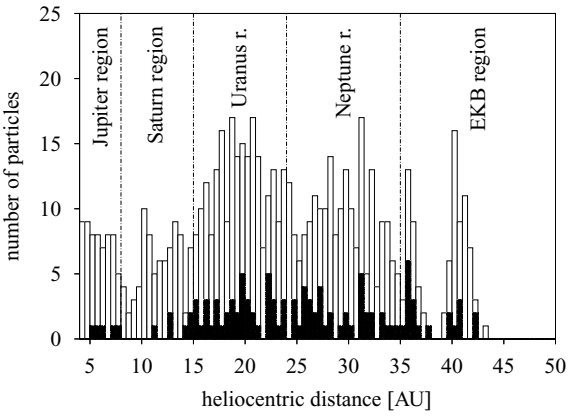

Figure 3. The numbers of the TPs moved into the inner OC from the Jupiter, Saturn, Uranus, Neptune and EKB regions. The full bars illustrate the numbers of the TPs in 0.5 au wide intervals of the initial PPD, which reside in the inner OC at 2 Gyr. The empty bars do so for the TPs ever occurring, at least for a short period, in the inner OC. (The animation of the evolution during the entire investigated period of this dependence as well as the dependencies shown in Figs 4–11 are available, in the *avi* format, at: http://www.ta3.sk/∼mjakubik/AstroDyn/INNER_OC_FORMATION/anims.php)

the solid curve in Fig. 4f). This value is almost consistent, within the determination uncertainty, with $s = -3.5$ found by Duncan et al. (1987) for the 3000–50 000 au interval, but at 4.5 Gyr. A different value of the index, $s = -2.9$, for this interval was found by Emel'yanenko, Asher & Bailey (2007), who, however, proceeded by a different way to model the OC than we and Duncan et al. The number of TPs increases with the highest rate in the interval from ≈3000 to ≈25 000 au (Fig. 5), i.e. in almost the whole region of the inner OC.

Fig. 6 shows the distribution of the semimajor axis of the TPs, which are situated in the OC at 2 Gyr. Again, we show an interval of a larger than the inner OC. The existence of a smooth transition from the inner to the outer part of the comet cloud is evident. The a-distribution also demonstrates that the OC is centrally concentrated. The decrease in the innermost interval of 0–5000 au is caused by the existence of the inner limit of the cloud due to its definition, rather than to the lack of TPs. We found that the behaviour in the range 5000–50 000 au is best fitted with a power law with index $s_a = -1.736^{+0.038}_{-0.028}$.

The information contained in the distribution of the semimajor axis is completed with the information in the distribution of eccentricity of the inner-OC orbits at 2 Gyr, which can be seen in Fig. 7. At 2 Gyr, a prevailing part of TPs in the inner OC moves on highly eccentric orbits. One can note that the eccentricities lower than about 0.2 are missing. The animation of the entire evolution of this distribution (fig07.avi) confirms the expected fact that the TPs come to the inner OC on highly eccentric orbits, with $e \to 1$. Due to the periodic variation of this element, which is coupled with the periodic variation of the perihelion distance (Neslušan & Jakubík 2005, fig. 4; see also Byl 1986; Heisler & Tremaine 1986; Pretka & Dybczyński 1994), some values of e lower than 0.98 begin to appear after 30 Myr. Then, the lower and lower values of the eccentricity start to appear. The down limit of ≈0.2 is reached after about 500 Myr. During the 500–2000 Myr period, the values lower than 0.2 also occur, but only sporadically and for a short time. The typical distribution during this period is similar to that at 2 Gyr shown in Fig. 7.

2.4 The orientation of the inner-OC orbits

In our computation, we used the non-rotating galactic coordinate frame. The initial orientation was chosen to be identical to the current orientation. In the presented figures, we still use this orientation enabling a simple transformation between the galactic and ecliptic coordinate systems. This fact is necessary to be kept in mind if one wanted to relate a structure to the position of the Galactic Centre or solar apex, which are uncertain in the given context. To indicate the difference between the used and regular galactic frames, we refer the used frame as 'zero-time galactic coordinate frame', hereinafter.

The distributions of the angular orbital elements of the TPs being still in the inner OC at the end of the simulation (at 2 Gyr) are shown in Fig. 8 both zero-time galactic and ecliptical coordinate systems. Because of the relative small population of the TPs in the inner OC at a given time, the height of the bars in the plots varies, when the plots are constructed for several, not very different times (e.g. 1960, 1980, 2000 Myr). However, in all such mutually corresponding plots, we can see, in the zero-time galactic coordinates (left-column plots): (i) a very high peak at $80^\circ \lessapprox i \lessapprox 90^\circ$ and the zero-value or close-to-zero-value minima at $i \lessapprox 55^\circ$ and $i \gtrapprox 100^\circ$ in plot (a) (see also animation fig08a.avi), (ii) the maxima at 90°–180° and 260°–320° intervals and the minima at 0°–60° and 180°–220° intervals in plot (c) and (iii) the high maximum at 160°–180° interval (a wider maximum in 140°–200°) and minimum in 220°–340° interval at plot (e).

The corresponding features can be seen in the distributions constructed in the ecliptical coordinate system (right-hand column plots of Fig. 8). Seeing the plot showing the ecliptical distribution of the argument of perihelion, ω_e (Fig. 8d), or the corresponding animation (fig08c.avi) from ≈300 Myr, the maxima in this distribution are related to the initial values in quadrants, approximately, centred at 0° and 180°, in which the perihelia of the largest number of TPs were detached from the planetary region by the Galactic tide. Another information about the directional distribution of bodies in the inner OC can be deduced from Fig. 9, illustrating the directions of their aphelion points.

All plots in Figs 8 and 9 document the expected scenario of the formation of the OC inner part. At the beginning (see also animation fig09b.avi), the comets are delivered to the inner OC on orbits with a very low inclination to the ecliptic. The Galactic tide is mostly efficient when acting on the orbits with the aphelia in large distances (also large angular distances) from the Galactic–equator plane (Galactic z-component of the aphelion point is large). So, these orbits are soon changed by the tide. The tide is less efficient in the case of comets approaching the inner OC on orbits with aphelia close to the Galactic–equator plane. Here, the process of their change is relatively slow. Some orbits with a low inclination to both ecliptic and Galactic equator can be seen surviving in a relatively low galactic-latitude region ($-45^\circ < b < +45^\circ$) in Fig. 9(a). In the region that is between approximately -45° and $+45^\circ$ in b and that is also far from the ecliptic, there are almost no aphelia.

We suggest that there is no sufficient mechanism to change the orbits in the way their aphelia would appear in this interval of b and far from the ecliptic, at the same time. The secondary outer perturbers are, probably, too weak to change the orbits so much. Taking into account both the absence of the aphelia in the galactic-latitude interval from -45° to $+45^\circ$ and far from the ecliptic (Fig. 9a) and the absence of aphelia above the ecliptic latitude $\beta \approx +60^\circ$ and below $\beta \approx -60^\circ$ (Fig. 9b), we can deduce the following. The dominant z-term of the Galactic tide is known to cause the cyclic change of Galactic inclination only from a limiting (mostly different from 90°)

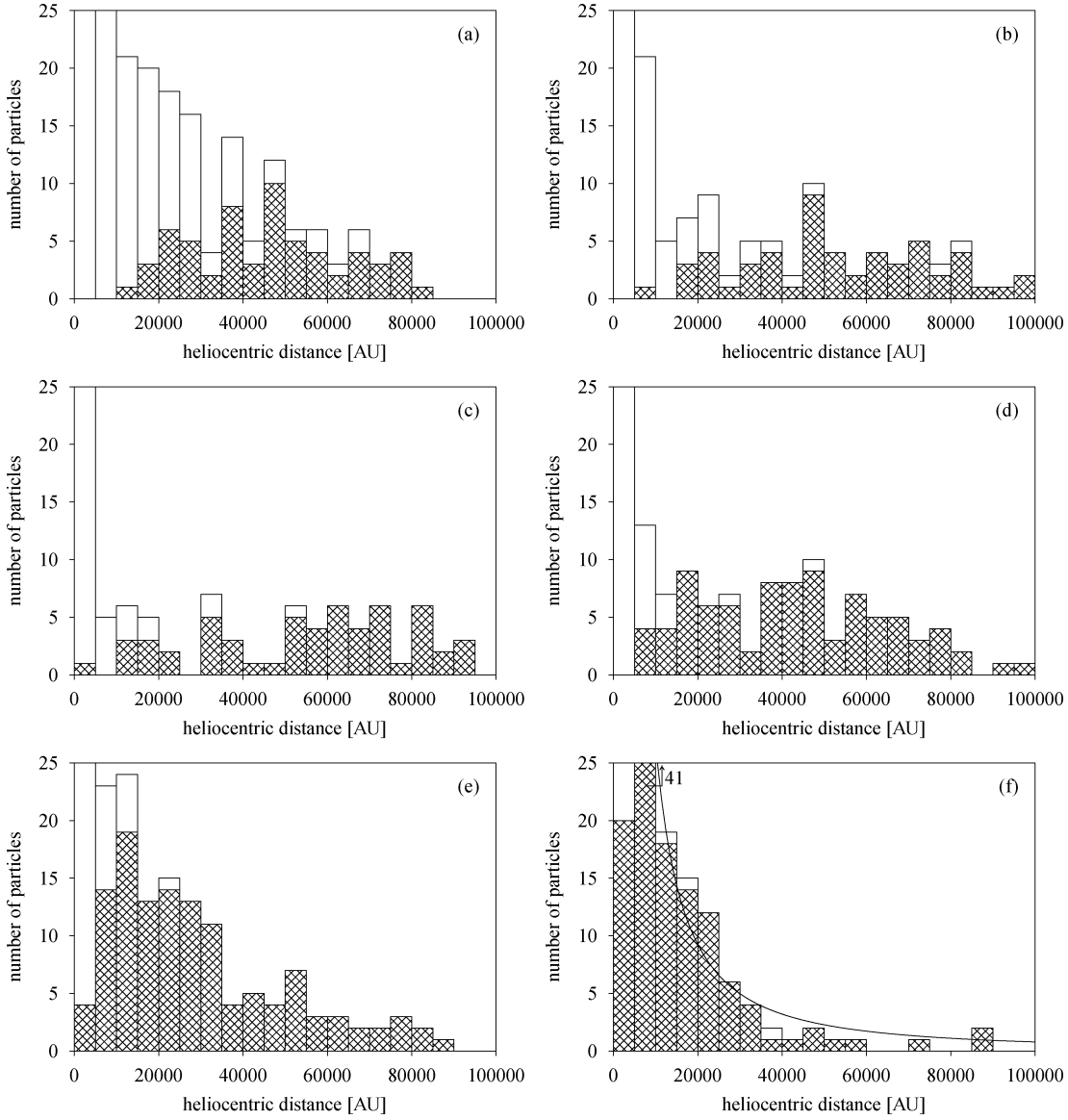

Figure 4. Distributions of OC comets (cross-hatched bars) for the times of 2 (plot a), 8 (plot b), 31 (plot c), 125 (plot d), 500 (plot e) and 2000 Myr (plot f) are shown. The distributions of all comets still bound to the Sun, for the same times, are also shown (empty bars). The vertical-axis scale is well suited to show the OC comets distribution that causes the second distributions (empty bars) are 'cut' for $r < 10\,000$ au. In plot f, the bar for $5000 < r < 10\,000$ au is also out of the range; the actual value is given. When all comets in the given interval are in the OC, the cross-hatched bar overlaps the empty bar. In plot f, data between 5000 and 100000 au are best fitted with a power law with index $s = -1.53$ (see solid line).

value to a value approaching 90° in the same quadrant. We know that the variation of the galactic inclination is coupled with that of the perihelion distance, whereby the inclination approaches its limiting value just at the moment when the perihelion distance is at the minimum of its periodic-variation cycle. This is also the case, when the TPs are escaping from the planetary region. Let us stress here that such escape is due to the planetary perturbations only, which cause the semimajor axis (and consequently the aphelion distance) to grow enough to allow the Galactic tide do start its action (but leaving the perihelion distance mostly unchanged). At this point, the inclination to the ecliptic is still small. Thus, a TP starting its motion to the inner OC should be on an orbit with the galactic inclination close to the limiting value. At the same time, the inclination to the ecliptic, which is inclined to the Galactic equator by 60.°2, is very low. Thus, the galactic inclination can typically librate only within the interval from the limiting value to 90°. The limiting value is not much different from 60.°2. In the ecliptic coordinate frame, the inclination can vary, due to the described mechanism, from 0° to ≈ 30° resulting in the ecliptic-latitude variation of the aphelion points from roughly −30° to +30°. This implies a certain significance of the secondary outer perturbers, too, since we observe (Fig. 9b) also some aphelia in the intervals of β from +30° to +60° and from −60° to −30°, approximately.

As mentioned in Paper I, the Galactic inclination of orbits with the very short perihelia in the minimum of the libration cycle of this element approaches the value of 90° for a relatively long period due to the action of the dominant, z-term of Galactic tide. Therefore, the probability of the occurrence of an orbit with a very high Galactic inclination is high. This can explain the high peak in the 80°–90° interval in Fig. 8(a) (or in the 25°–35° interval in Fig. 8(b),

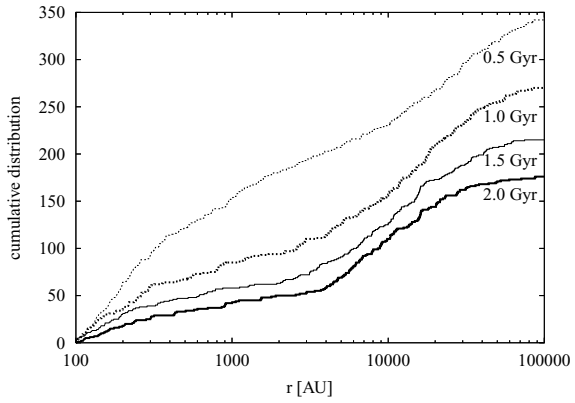

Figure 5. The cumulative distribution of all TPs situated in the interval of heliocentric distances between 100 and 100 000 au after 500, 1000, 1500 and 2000 Myr.

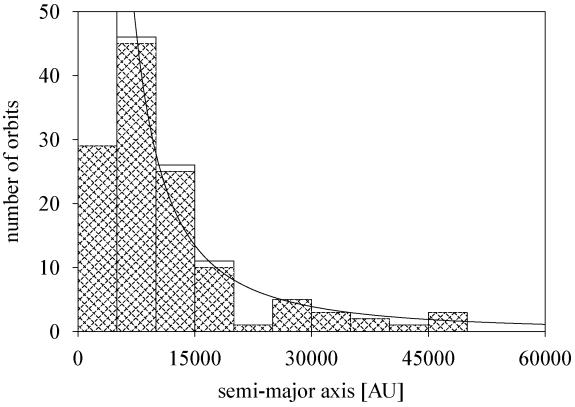

Figure 6. Distribution of the orbital semimajor axis of TPs residing in the OC at 2 Gyr (cross-hatched bars). The corresponding distribution of all comets, still bound to the Sun, is also shown (empty bars). In the interval from 5000 to 50 000 au, the OC comet semimajor axis distribution is fitted by the power law with the index of slope $s_a = -1.74$ (solid curve).

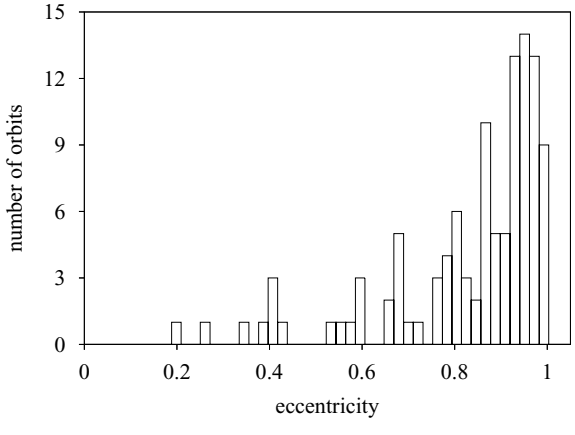

Figure 7. Distribution of the orbital eccentricity of TPs residing in the inner OC at 2 Gyr.

with respect to the angle between the ecliptic and Galactic–equator planes).

In the case of inner OC, the magnitudes of the action of outer perturbers are weaker than the corresponding magnitudes in the case of outer OC. It is, therefore, not surprising that the described distributions of the orbital elements of the TPs situated in the inner OC imply a large inhomogeneity in the structure of the whole part of this cloud even after 2 Gyr lasting evolution. In 2 Gyr, the inhomogeneity is, however, not longer caused by the origin of the TPs in a flat PPD. The initial dynamical memory is forgotten and the actual dynamics is governed, in particular, by the dominant, z-term of the Galactic tide. Though the outer perturbers are inefficient to completely thermalize even the most distant part of the inner OC, they seem to be efficient enough to significantly change a prevailing part of its orbits.

At the end of this section, let us rise some questions. How are all the characteristics of the inner OC we found at the end of the simulated 2 Gyr related to the current structure of this part of the comet cloud? Can the largest periods of element variations of the innermost orbits in the inner OC, not covered by our simulation, cause some significant differences between the overall pictures of the inner OC at 2 Gyr and at present? In the related animations (fig05.avi–fig12b.avi), the general features are more or less stable since the time the population of the inner OC reaches its maximum (1250 Myr). The period from 1250 to 2000 Myr is, however, relatively short, therefore we should be careful when extrapolating the result from this period to the whole subsequent period from 2 Gyr till present (4.5 Gyr). A radical change of the inner-OC structure can hardly be expected, yet. We, however, cannot exclude a quantitative change due to a slow, but permanent dynamical evolution.

2.5 The flatness of the trans-Neptunian belt and inner OC

No empty regions exist between the populations of small bodies beyond the orbit of Neptune. The division into the EKB, scattered disc, extended scattered disc and inner OC is established only for our methodological purpose. The trans-Neptunian disc, containing the objects on orbits with a low inclination to the ecliptic, is expected to smoothly expand into a lesser and lesser flat region and gradually become a spherical comet cloud. In this section, we attempt, on the basis of our simulation, to answer the question of how quickly the low inclination of the disc-object orbits to the ecliptic disappears and at what heliocentric distance the more or less spherically symmetric comet cloud occurs.

We know that the orbits of bodies in the EKB have a low inclination to the ecliptic (typically up to 40°). Our question on the flatness of the trans-Neptunian population concerns the most distant regions, in particular. The distribution of the TPs, having their semimajor axes in the interval $50 < a < 25\,000$ au in the i–a phase space, is illustrated in Fig. 10. More exactly, the upper a in the upper plot is 22 000 au, since there is no TP with a between 20 490 and 25 280 au. We can see that the larger and larger values of the inclination occur with the increasing semimajor axis. The disc departs, step by step, from the ecliptic. The inclinations larger than $\approx 45^\circ$ occur for $a \gtrapprox 4000$ au and those larger than $\approx 90^\circ$ for $a \gtrapprox 8500$ au.

An interesting phenomenon is an almost disappearance of the TPs with $i \lessapprox 20^\circ$ for $a \gtrapprox 5500$ au. This phenomenon is likely to be due to the geometry of the initial appearance of bodies in the inner OC and to very long periods of the variation of inclination in this part of the OC. The bodies are delivered there on a close-to-zero inclination to the ecliptic. This value corresponding to the minimum of the inclination libration cycle caused by the Galactic tide is changed relatively quickly in a first stage (newly coming bodies move only a short time on orbits with $i \to 0^\circ$), but very slowly later. The time of 2 Gyr (or shorter in the case of TPs coming into the inner OC in later time) appears to be too short to complete

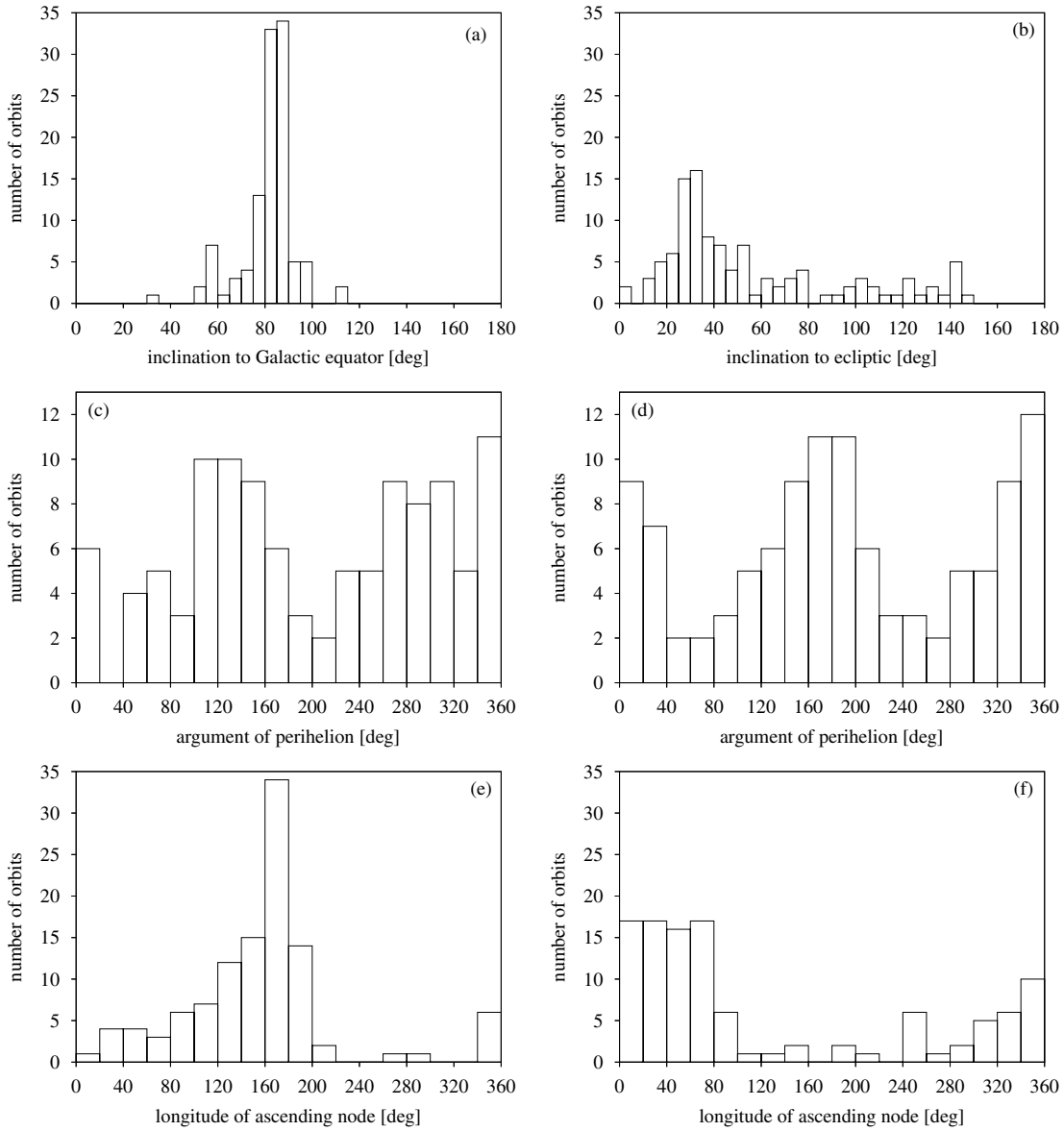

Figure 8. Distributions of angular elements of TPs residing in the inner OC at 2 Gyr. The left-hand column plots demonstrate the distributions in the zero-time galactic coordinate frame, the right-hand column plots in the ecliptic coordinate frame. The pairs of plots (a) and (b), (c) and (d) and (e) and (f) show the distribution of the inclination (to the Galactic plane or ecliptic), argument of perihelion and longitude of ascending node, respectively. Note the different vertical scale.

the entire libration cycle and return the inclination below the value of 20°.

For $a \gtrapprox 10\,000$ au, the inclination to the ecliptic fills the entire interval from ≈20° to ≈150°. However, it does not exceed ≈150° even at the outer border of the inner OC. The reason for this phenomenon is obviously the same as that discussed in the description of Fig. 9 in Section 2.4. The absence of orbits with the ecliptical $i \gtrapprox 150°$ and $i \lessapprox 20°$ (the latter for $a \gtrapprox 5500$ au) implies that the inner OC is not spherically symmetric in any part, and this fact does not allow us to perform a more exact evaluation of the trans-Neptunian disc flatness, with the most exactly determined characteristics.

The spatial flatness of the trans-Neptunian disc can be better seen in the distribution of the ecliptical z-component of the TPs at the final time of the simulation (Fig. 11). Although the number of TPs in the critical intervals of heliocentric distance, r, in which the flatness starts to disappear is small, we can conclude, seeing a more central region $r < 5000$ au (Fig. 11b), that the part of the disc in the region of $r \lessapprox 1000$ au is clearly situated nearly the ecliptic. Beyond this (but possibly $r \approx 1500$ au) distance, more TPs are situated at a larger distance from the ecliptic. The magnitude of TPs' z-component seems to fill the whole interval from 0 to r only in the region between $3000 \lessapprox r \lessapprox 6000$ au, therefore our simulation does not exclude a cloud that could, practically, be spherically symmetric in this interval (but it does not either prove the symmetry due to poor statistics). Beyond $r \approx 6000$ au, the TPs situated directly above and below the Sun (with respect to the ecliptic) are missing. This absence is obviously linked to the absence of orbits with $i \gtrapprox 150°$.

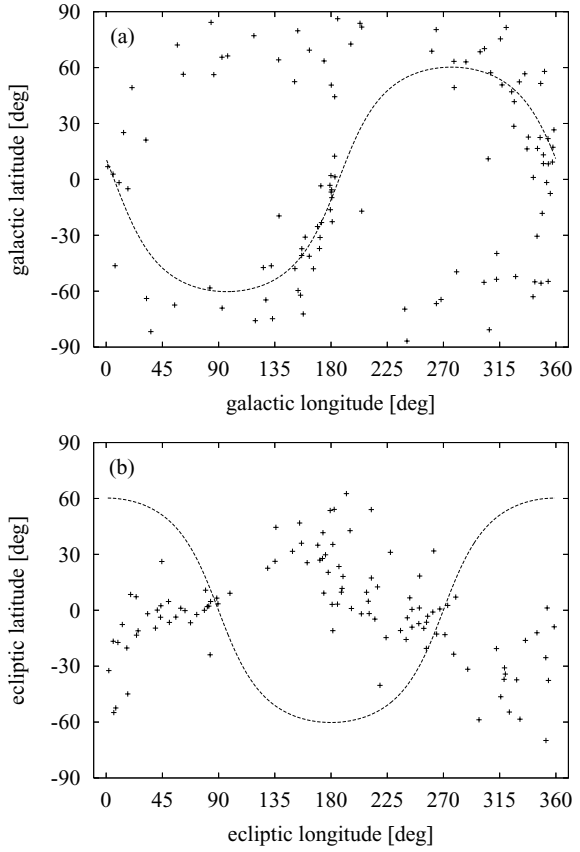

Figure 9. Directional distribution of the aphelion points of TPs residing in the inner OC at 2 Gyr. Plot (a) shows the distribution in the zero-time galactic coordinate frame and plot (b) does this in the ecliptic coordinate frame. The dashed curve shows the position of the ecliptic in plot (a) and Galactic Equator in plot (b).

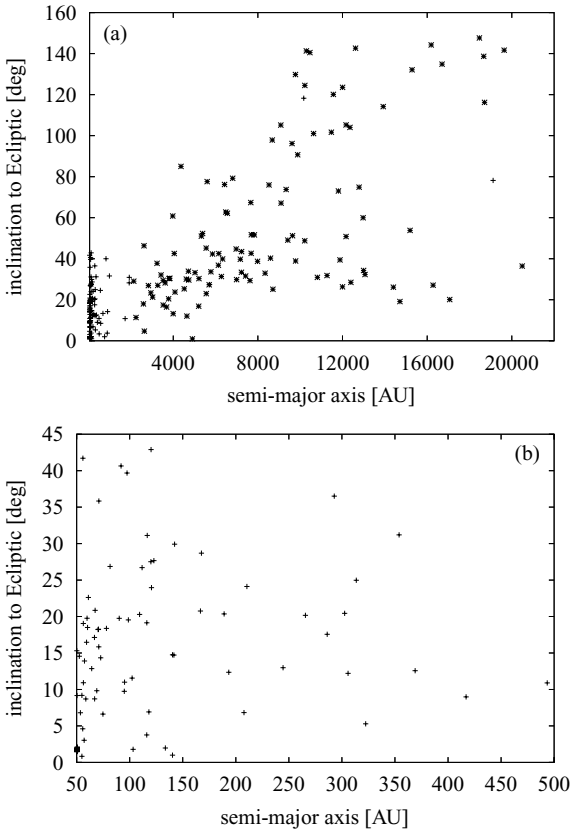

Figure 10. Inclination to the ecliptic versus semimajor axis of the TPs on the orbits with semimajor axis in the interval $50 < a < 22\,000$ au (plot a) and $50 < a < 500$ au (plot b) at 2 Gyr. The TPs residing in this time in the inner OC are shown with asterisks, the other TPs with crosses.

3 SUMMARY

Considering the model of the PPD consisting of 10 038 TPs and perturbations by four giant planets on their current orbits and with their current masses, as well as the perturbations by the Galactic tide and passing stars, we simulated the formation of the OC and the accompanying dynamical evolution of the EKB during the first 2 Gyr. In this paper, we dealt with the inner OC, in particular. For the last 0.75 Gyr period, the general structure of the inner OC and adjacent regions does not significantly change, but one must be careful when extrapolating the structure for 2 Gyr to the present cloud. Though slowly, it has still evolved during another 2.5 Gyr, therefore some differences could appear. Modelling the formation of the comet reservoirs, we can state the following about the model of the inner OC.

(i) The inner-OC population quickly rises during the first mega-year due to the ejections of TPs from the Jupiter–Saturn region (Fig. 1). However, after reaching a very early maximum, it steeply decreases. From few mega-years after the beginning, it again increases till the maximum at about 1250 Myr. From this time, an erosion of the inner OC has dominated over an increase in its population.

(ii) Dividing the TPs in the inner OC by the region of their origin, we can conclude that the largest amounts originate from the Uranus and Neptune regions: 35.5 and 35.4 per cent, respectively. The amount of the TPs originating in the EKB region appears to be larger than each of the amounts from the Jupiter and Saturn regions starting from ≈500 Myr, and clearly exceeds these amounts at 2 Gyr. At this time, there are 4.5, 6.3 and 18.4 per cent TPs originating in the Jupiter, Saturn and EKB regions, respectively, in the inner OC.

(iii) According to our simulation and definitions of the inner and outer OC, only about 10 per cent of the TPs, that are in the OC at 2 Gyr, reside in the outer OC. The formation efficiency of the inner OC is 1.1 per cent.

(iv) At 2 Gyr, the number density of the TPs residing in the OC in the interval $5000 < r < 100\,000$ au can be fitted by the power law with the index of slope $s = -3.529^{+0.031}_{-0.024}$. The distribution of the semimajor axis in the 5000– 50 000 au interval can also be approximated by the power law with the index $s_a = -1.736^{+0.038}_{-0.028}$. The distribution of eccentricity of the inner-OC orbits implies that a prevailing part of TPs in the inner OC moves on highly eccentric orbits. The eccentricities lower than about 0.2 are almost missing.

(v) Even after 2-Gyr evolution, the orientation of the inner-OC orbits is strongly inhomogeneous. It can especially be seen in the distributions of the zero-time-galactic angular elements (Fig. 8). At 2 Gyr, the inhomogeneity is not, however, caused by the origin of the TPs in a flat PPD. The initial dynamical memory is forgotten and the actual dynamics is governed by the dominant z-term of the Galactic tide in particular.

(vi) The orbits in the innermost part of inner OC have a low inclination to the ecliptic as expected. Compared to the semimajor axis, the inclinations larger than $\approx 45^\circ$ occur for $a \gtrapprox 4000$ au and those larger than $\approx 90^\circ$ for $a \gtrapprox 8500$ au. The actual location of

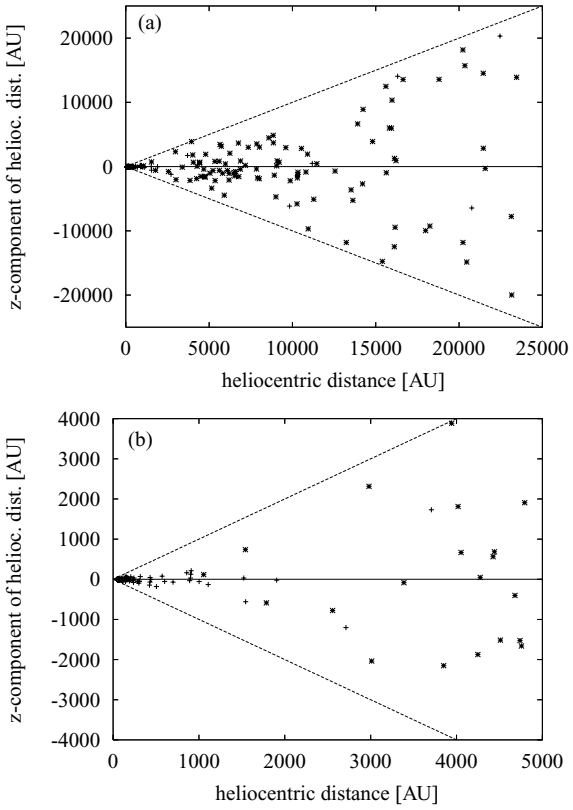

Figure 11. Occurrence the TPs above and below the ecliptic. Specifically, the ecliptical z-component of heliocentric distance versus this distance of the TPs is shown, at 2 Gyr. In more detail, the TPs up to outer border of the inner OC are demonstrated. Plot (a) demonstrates the z versus r distribution for $50 < r < 25\,000$ au and plot (b) is a more detailed view of the $50 < r < 5000$ au interval. The TPs residing at 2 Gyr in the inner OC are shown with asterisks, the other TPs with crosses. Since $|z| \leq r$, no TP can occur above the upper and below the lower diagonals.

the TP position near the ecliptic (low magnitude of ecliptical z-coordinate) is apparent in the interval of heliocentric distance up to $\approx$1000 au. Beyond the distance of $\approx$6000 au, the TPs are also abundant at large distances from the ecliptic, except for the region directly above and below the Sun, with respect to the ecliptic.

ACKNOWLEDGMENTS

GL thanks PI2S2 Project managed by the Consorzio COMETA, http://www.pi2s2.it and http://www.consorzio-cometa.it for the computational resources and technical support. MJ, TP and LN thank the project 'Enabling Grids for E-sciencE II' (http://www.eu-egee.org/) for the provided computational capacity and support in the development of the computer code, which was necessary for the management of tasks on the GRID. They also acknowledge the partial support of this work by VEGA – the Slovak Grant Agency for Science (grant no. 7047). PAD acknowledges the partial support of this work from Polish Ministry of Science and High Education (year 2008, grant no. N N203 302335).

REFERENCES

Bahcall J. N., 1984, ApJ, 276, 169
Byl J., 1986, Earth Moon Planets, 36, 263
Crézé M., Chereul E., Bienaymé O., Pichon C., 1998, A&A, 329, 920
Dones L., Weissman P. R., Levison H. F., Duncan M. J., 2004, in Festou M. C., Keller H. U., Weaver H. A., eds, Comets II. Univ. Arizona Press, Arizona, p. 153
Duncan M., Quinn T., Tremaine S., 1987, AJ, 94, 1330
Dybczyński P. A., 2001, A&A, 375, 643
Dybczyński P. A., 2006, A&A, 449, 1233
Dybczyński P. A., Leto G., Jakubík M., Paulech T., Neslušan L., 2008, A&A, 487, 345
Emel'yanenko V. V., Asher D. J., Bailey M. E., 2007, MNRAS, 381, 779
Heisler J., Tremaine S., 1986, Icarus, 65, 13
Hills J. G., 1981, AJ, 86, 1730
Holmberg J., Flynn C., 2000, MNRAS, 313, 209
Neslušan L., Jakubík M., 2005, A&A, 437, 1093
Pham H. A., 1997, in Perryman M. A. C., Bernaca P. L., eds, *Hipparcos* Venice 97. ESA-SP 402. ESA Publications Division, Noordwijk, p. 559
Pretka H., Dybczyński P. A., 1994, in Kurzyńska K., Barlier F., Seidelmann P. K., Wytrzyszczak I., eds, Dynamics and Astrometry of Natural and Artificial Celestial Bodies. Astronomical Observatory of A. Mickiewicz Univ., Poznań, p. 299

This paper has been typeset from a TEX/LATEX file prepared by the author.